Structural Analysis of ARC-Type Inhibitor (ARC-1034) Binding to Protein Kinase A Catalytic Subunit and Rational Design of Bisubstrate Analogue Inhibitors of Basophilic Protein Kinases

Darja Lavogina,[†] Marje Lust,[†] Indrek Viil,[†] Norbert König,[‡] Gerda Raidaru,[†] Jevgenia Rogozina,[†] Erki Enkvist,[†] Asko Uri,*,[†] and Dirk Bossemeyer[‡]

Institute of Chemistry, 2 Jakobi Street, 51014 Tartu, Estonia, Group of Structural Biochemistry, German Cancer Research Centre, Im Neuenheimer Feld 280, 69120 Heidelberg, Germany

The crystal structure of a complex of the catalytic subunit (type α) of cAMP-dependent protein kinase (PKA Cα) with ARC-type inhibitor (ARC-1034), the presumed lead scaffold of previously reported adenosine-oligo-arginine conjugate-based (ARC-type) inhibitors, was solved. Structural elements important for interaction with the kinase were established with specifically modified derivatives of the lead compound. On the basis of this knowledge, a new generation of inhibitors, conjugates of adenosine-4′-dehydroxymethyl-4′-carboxylic acid moiety and oligo(D-arginine), was developed with inhibitory constants well into the subnanomolar range. The structural determinants of selectivity of the new compounds were established in assays with ROCK-II and PKBγ.

Introduction

Protein kinases (PKs[a]) belong to the transferase class of enzymes and constitute a large gene family comprising ca. 2% of the mammalian and 4% of the plant genome.[1,2] Their common function, catalysis of protein phosphorylation, is a key mechanism of cell regulation, switching cellular systems as responses to extra- and intracellular stimuli.[3] Aberrant activity of PKs due to mutation, overexpression, or disabled cellular inhibition can result in serious diseases including diabetes, cancer, and immune system deficiencies;[4,5] some protein kinases contribute to disease also during their normal cellular functioning. Because of the established important role of kinases in tumor genesis and progression more than 70 small-molecule kinase inhibitors are at various stages of clinical trials as anticancer drugs.[6]

Consequently, a considerable amount of research is dedicated to the development, screening, and improvement of protein kinase inhibitors. The most common type of inhibitors is ATP-site directed.[7−9] They have generally good affinity characteristics, but their selectivity suffers from the high homology of ATP-binding sites of protein kinases.[10,11] Other target sites have been explored,[12] and recently several highly selective peptide-based inhibitors have been developed;[13,14] for nanomolar potency, however, longer peptidic structures are required, making cellular transport and stability of the compounds an issue.

Bisubstrate-analogue, or biligand inhibitors target both the binding site for the cosubstrate ATP and the binding site for the substrate protein/peptide. For this they combine two inhibitory domains, each mimicking one of the substrate types, and simultaneously associate with binding sites of both substrates. First applied to the adenylate kinase in 1972,[15] such a bisubstrate-analogue inhibitor approach has given several potent inhibitors of protein kinases.[12,16] Variations have addressed both the structures of the incorporated single-site inhibitors/pseudosubstrates and the linking chain. The principle advantage of bisubstrate-analogue inhibitors is their potential for a synergistic effect on affinity compared to the affinities of the single components[17,18] due to entropic and enthalpic factors. The additional prospect of a possible higher tolerance of such systems toward mutations of the so-called gate-keeper residue, a major factor in the emergence of therapy resistance, has been suggested.[19]

Previously, we reported the development of conjugates of oligo-(D-arginine) peptides with adenosine-4′-dehydroxymethyl-4′-carboxylic acid (ARCs), 5-isoquinolinesulfonic acid,[7] or carbocyclic analogue of 3′-deoxyadenosine.[20] These compounds are highly potent inhibitors of protein kinase A (also known as cAMP-dependent protein kinase, cAPK or PKA) with inhibitory constants in the low nanomolar region. This high potency of the conjugates contrasts to merely submillimolar activities of their individual single site-targeted constituents. This is an indication of the true bisubstrate character of the inhibitors, although kinetic analysis reveals competitiveness with only one substrate, ATP. The bisubstrate functioning was further confirmed in surface plasmon resonance binding studies, showing a competitive displacement of the compounds from their complex with the kinase by ligands targeting either the ATP-

---

* To whom correspondence should be addressed. Phone: +3725175593. Fax: +3727375275. E-mail: asko.uri@ut.ee.
† Institute of Chemistry.
‡ Group of Structural Biochemistry, German Cancer Research Centre.

[a] Abbreviations: Abu, 4-aminobutanoic acid moiety; Adc, adenosine-4′-dehydroxymethyl-4′-carboxylic acid; Ahx, 6-aminohexanoic acid moiety; AMP-PNP, adenylyl-5′-imidodiphosphate; Aoc, 8-aminooctanoic acid moiety; ARC, adenosine−arginine conjugate; BisTris, 1,3-Bis[tris(hydroxymethyl)methylamino]; Boc, *tert*-butoxycarbonyl; BOP, benzotriazol-1-yl-oxytris(dimethylamino)-phosphonium hexafluorophosphate; Bz, benzyl; Bzo, benzoyl; DCE, 1,2-dichloroethane; DIEA, diisopropylethylamine; Fmoc, 9-fluorenylmethoxycarbonyl; GST, glutathione S-transferase; H1152P, (S)-(+)-4-methyl-5-(2-methyl-[1,4]diazepane-1-sulfonyl)-isoquinoline; H89, N-[2-((p-bromocinnamyl)amino)ethyl]-5-isoquinolinesulfonamide dihydrochloride; HOBt, N-hydroxybenzotriazole; MALDI-TOF, matrix-assisted laser desorption/ionization-time-of-flight; MBHA, 4-methylbenzhydrylamine; Mes, 2-(N-morpholine)-ethanesulfonic acid; MS, mass spectrometry; PDB, Protein Data Bank; PK, protein kinase; PKA, cAMP-dependent protein kinase; PKA Cα, cAMP-dependent protein kinase catalytic subunit type α; PKBγ, protein kinase B isoform type γ (Akt3); PKI, heat-stable protein kinase inhibitor; RIIα, cAMP-dependent protein kinase regulatory subunit isoform IIα; ROCK-II, GST-tagged Rho-dependent protein kinase; TAMRA, carboxytetramethylrhodamine; TEA, N-triethylamine; TFA, trifluoroacetic acid.

binding pocket (such as ATP, H89, or H1152P) or the protein–substrate-binding site (RIIα and GST-PKIα).[21] Further, the selectivity profiling with a wide kinase panel (altogether 52 kinases) revealed a strong tendency of the arginine-rich conjugates to inhibit basophilic PKs, corresponding to an active contribution of both functional moieties in the formation of the binary complex with the kinase.[7,20]

Protein kinases share the bilobal overall structure of a highly conserved catalytic core, although details of ligand binding patterns and recognition sites are different.[22,23] PKA that was used as the target protein kinase in this work is one of the best characterized protein kinases. Its structural similarities to certain other protein kinases led to its use as an "ersatz"-kinase, e.g., structural models in the form of chimeras can be constructed carrying specific point mutations to mimic inhibitor binding sites of related kinases.[24,25] Protein kinase A α-catalytic subunit (PKA Cα) has been crystallized as an apoenzyme and cocrystallized in a variety of complexes with a peptide derived from the pseudosubstrate inhibitor PKI, with protein kinase C inhibitors,[26] Rho-kinase inhibitors,[24,27] general PK inhibitors like staurosporine[28] and Hidaka's inhibitors,[27,29] and a variety of balanol derivatives.[30,31] Here we present the crystal structure of the complex of the catalytic subunit of PKA with a representative of ARC-type inhibitors, the compound **1** (ARC-1034). To our knowledge, bisubstrate-analogue inhibitors have been so far cocrystallized with four target protein kinases, representing both tyrosine kinases (the core tyrosine kinase domain of the insulin receptor, at 2.7 Å resolution;[16] the epidermal growth factor receptor kinase domain, 2.6 Å resolution;[32] and Abelson tyrosine kinase, 1.8 Å resolution[33]), and serine/threonine kinases (CMGC family, cyclin-dependent kinase 2, 1.7 Å resolution[34]). A key feature of the compound **1** disclosed by the structure is the linker region connecting the nucleosidic part and the peptidic part of the molecule, which connects well to the protein kinase glycine flap by utilizing a conformational induced fit change, at the same time orienting the attached oligo-D-arginine peptide for positioning of distal inhibitor side-chains. On the basis of the insights from the crystal structure, a new generation of adenosine analogue–oligo-(D-arginine) inhibitors was designed, synthesized, and characterized in PKA, PKBγ, and ROCK-II inhibition and binding assays. For the best of these novel ARC compounds, inhibition constants in the subnanomolar range were determined.

Results and Discussion

General Crystallographic Data. The chemical structure of the compound **1** (Figure 1) used for crystallization as the lead compound representing ARC-inhibitors was optimized on the basis of PKA inhibitory potential during previous studies.[7]

The compound **1** is a conjugate of adenosine-4′-dehydroxymethyl-4′-carboxylic acid moiety (Adc) and a D-arginine dipeptide linked by 6-aminohexanoic acid moiety (Ahx). The IC_{50} value of 2.6 μM (at 100 μM ATP) was determined in a PKA inhibition fluorometric TLC assay.[35]

The general crystallographic data of the PKA Cα–compound **1** complex (3BWJ) are presented in Table 1 and the electron density maps of the inhibitor binding pockets in Figure 2.

The complex crystallized in space group $P2_12_12_1$ to a resolution of 2.29 Å. This space group is common for various complexes of PKA, including those with the PKI(5−24) inhibitor peptide. The unit cell dimensions are minimally smaller (71.6/73.2/78.0 Å) than for typical PKA/PKI(5−24) complexes (PDB 1YDS: 73.6/76.3/80.6 Å).

The electron density map indicated the presence of the two compound **1** molecules bound to the kinase molecule (PDB
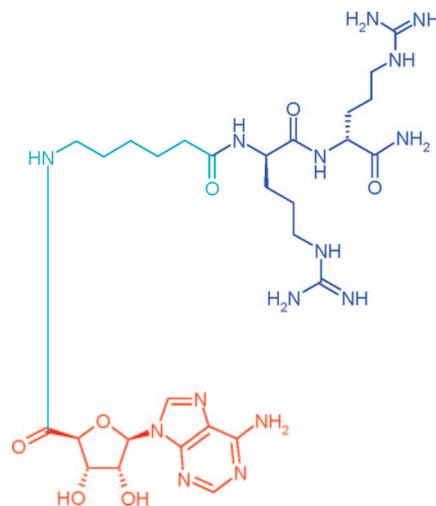

Figure 1. The structure of the compound **1**. The nucleosidic moiety is in red, the linker in cyan, and the peptidic moiety in blue.

Table 1. General Crystallographic Data of PKA Cα–Compound **1** Complex

data collection	
X-ray source	Deutsches Elektronen Synchrotron BW6, Hamburg
space group	$P2_12_12_1$
cell dimensions (a, b, c) (Å)	71.6, 73.2, 78.0
resolution range (Å)	53.38−2.28
completeness (%) (last shell)	99.9 (100)
R_{sym} (last shell)	0.119 (0.387)
solvent (%)	48.31
refinement	
number of atoms used in refinement	3098
R factor (%)	0.199
free R factor (%)	0.249
free R factor value test size (%)	5.1
reflections used	17407
standard deviation from ideal values	
bond length (Å)	0.017
bond angles (deg)	1.598
temperature factors	
mean B value	25.27

BJW3, see also Supporting Information), locating one ("inner") molecule to the catalytic cleft and the ATP-binding site and the other ("outer") one to the surface of the enzyme in the region wedged between two symmetry related PKA molecules. The presence of the "outer" compound **1** molecule is most likely caused by high inhibitor concentration at crystallization conditions, and it is not related to the mechanism of inhibition. Interestingly, the surface-bound "outer" compound **1** molecule contacts two phosphoryl groups from enzyme residues, Thr197P from one enzyme molecule, and Ser139P from the symmetry mate. The electron density for the inner compound **1** molecule in the ATP-binding site allowed unambiguous modeling for the adenosine moiety and the 6-aminohexanoic acid linker group. The electron density for the peptidic part of the inhibitor, facing the opening of the catalytic cleft, was discontinuous but allowed to model the two arginine residues (Figure 3). The "outer" compound **1** molecule is more exposed to the solvent, lying near the loop between helices F and G of the C-terminal lobe with its adenosine moiety at the hydrophobic surface formed by Tyr229, Tyr235, Phe238, and Phe239, and one of the arginines interacting with the phosphoryl moiety of the auto-
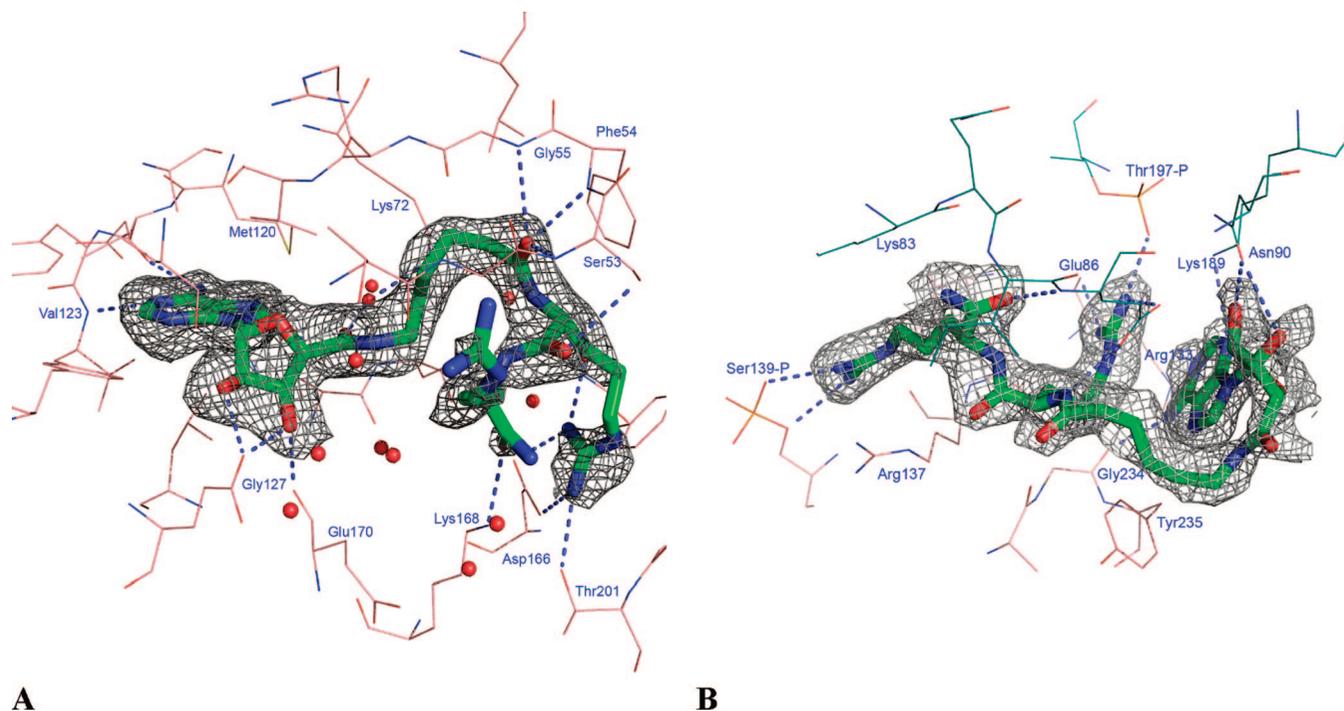
A   **B**

Figure 2. Electron density map within 1.6 Å around the compound **1** molecules contoured at 1 σ. (A) "Inner" compound **1** molecule in the active site. Enzyme residues of the binding site are shown with light red carbon atoms. H-bonds between the contacting groups of the inhibitor and the enzyme are depicted. (B) "Outer" compound **1** molecule in surface bound location. Residues of both symmetry mates within 4 Å from the inhibitor are shown. H-bond contacts are depicted. Symmetry molecules differ by light red or marine blue carbon atom colors. Figures were created with Pymol.
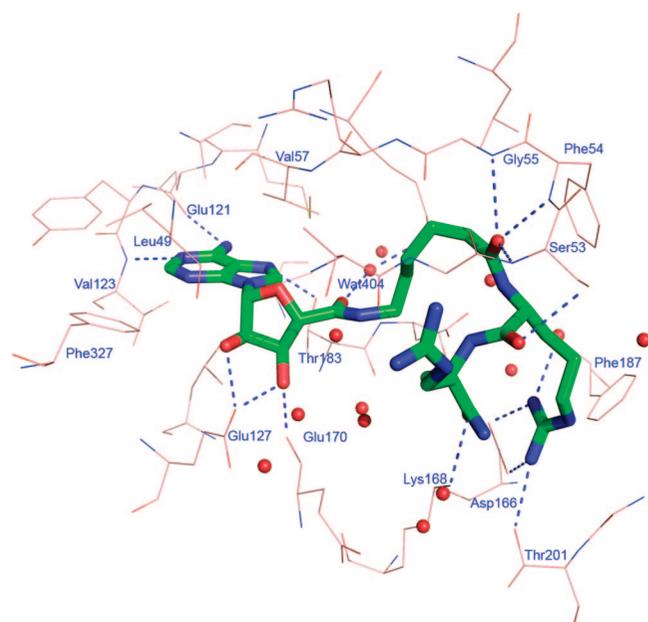

Figure 3. Interactions of the inner compound **1** molecule with amino acid residues of PKA. Enzyme carbons are light red, inhibitor carbons are in green. H-bonds are depicted. Water molecules are shown as red balls. Water 404 is noted.

phosphorylated Ser139 (Figure 4), the other one with the Thr197 phosphoryl group of a symmetry related kinase molecule.

The enzyme is in an active conformation, which can be considered intermediate (half-closed) because of the more open conformation of the glycine flap structure. While the open conformation of the glycine flap is often found among inhibitor cocrystal structures of protein kinases, the open position of the glycine flap in the PKA Cα−compound **1** structure is different from most of these as it is relatively well fixed, as indicated by

relatively low B-factors. The glycine flap appears to be fixed by interacting with the Ahx linker of the bound inner compound **1** molecule. With this, the overall structure is almost identical to the structure of the PKA complex with the isoquinoline sulfonamide inhibitor H89 and PKI(5−24) peptide (PDB 1YDT) with the rmsd value of 0.22 Å for Cα atoms. In 1YDT, the large bromocinnamyl side-chain binds to the glycine flap.[29]

Analysis of Interactions. The ATP-mimicking part of the inhibitor interacts with the enzyme as typical for an ATP molecule: Glu121 is an acceptor for the adenine N6-donated hydrogen bond, Val123 is a hydrogen bond donor for N1 of the purine ring, and the Thr183 hydroxyl group forms a H-bond to the purine N7. Also, the 2′ and 3′ hydroxyl groups of the ribose make typical contacts to the Glu127 side-chain and to the Glu170 backbone carbonyl. A new interaction, however, is formed between the O5′ oxygen of the carbonyl group connected to the C4′ of the ribose and water 404 in the ATP-binding site. This water molecule itself is well connected to the protonated amino group of the side-chain of Lys72 and to the hydroxyl group of Thr183. This indirectly connects O5′ to enzyme residues, thus possibly explaining the better inhibitory potency of conjugates containing an adenosine-4′-dehydroxymethyl-4′-carboxylic acid moiety, compared to conjugates with corresponding adenine and adenosine moieties, as was previously observed.[7]

A characteristic feature of the bound compound **1** molecule is the binding mode of the Ahx linker group. The main determinant is the interaction of the carbonyl O28 with the backbone amide groups of three residues from the glycine flap, Ser53, Phe54, and Gly55. Similar H-bond contacts have been observed in the complex with bound AMP-PNP or ATP between the β- and γ-phosphoryl groups and the same amide groups.[36,37] The flexible aliphatic chain of the linker packs underneath the glycine flap and makes van der Waals contacts with Val57. In
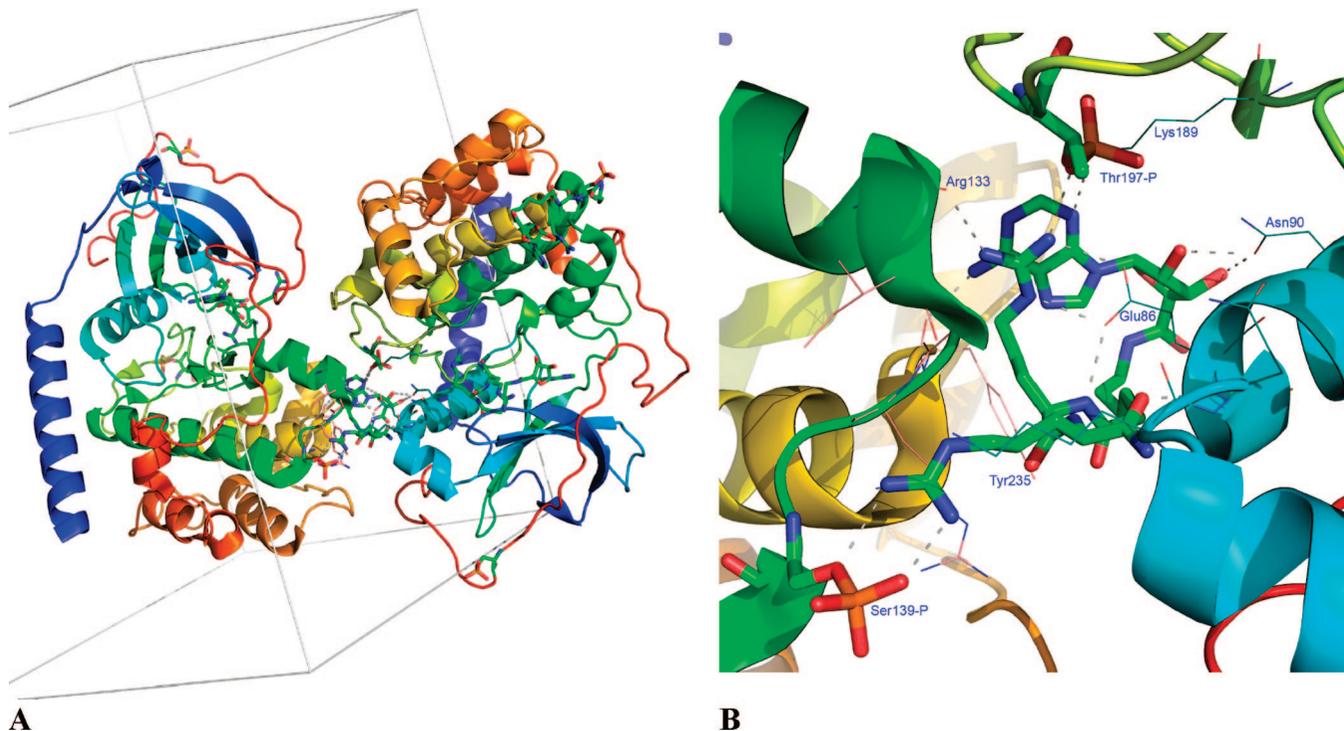
Figure 4. (A) Part of the unit cell showing two of the symmetry kinase molecules with bound compound **1** molecules. The interactions of the outer compound **1** molecule with the enzyme residues are indicated. (B) Binding site of the outer compound **1** inhibitor formed by two symmetry related enzyme molecules. H-bond interactions with the phosphoryl groups are shown. Symmetry molecules differ by color of carbon atoms (light red versus marine blue).
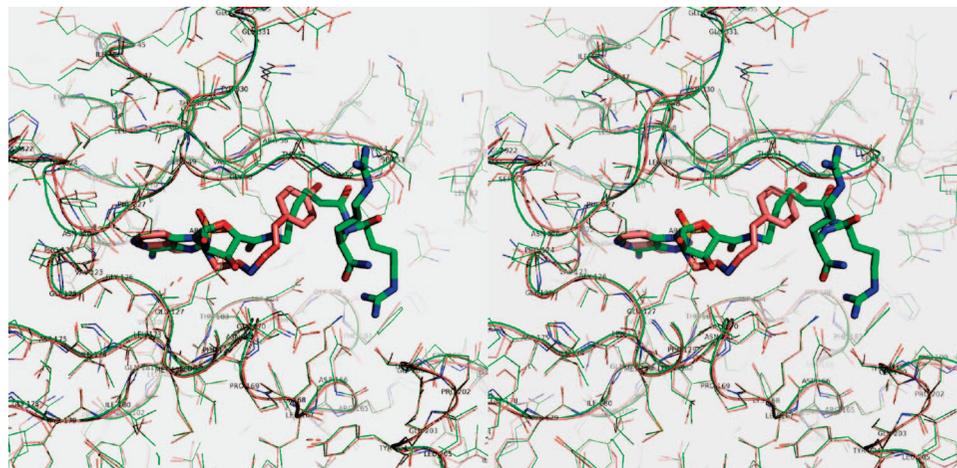

Figure 5. Overlay of structures in the region of the binding pockets of the compound **1** and H89 (1YDT). The compound **1** is shown with green carbon atoms, H89 with light red carbon atoms.

contrast to the AMP-PNP-complex, here the glycine flap is in a more open conformation, which may result from a fit of the flexible 6-carbon chain with the ribose on one side and the O28 position for multiple interactions with the backbone amides on the other side, accommodating the linker by a rotational movement of the glycine flap around a hinge defined by the C-α atoms of residues Gly50 and Val57. In this respect, the conformation of the glycine flap very much resembles the structure of 1YDT (H89 bound to PKA), whereas H-bonds with O28 replace hydrophobic interaction of the bromine atom with the glycine flap in 1YDT (Figure 5).

In contrast to the very good definition of the electron density for the nucleosidic part and for the aliphatic nonpolar flexible linker part of the "inner" compound **1** molecule, the electron density for the peptidic moiety is not continuous. This most likely indicates conformational mobility of the arginine residues.

The terminal distal arginine residue is exposed to the solvent and does not appear to make significant contacts to enzyme residues, with the exception of an H-bond from its carboxyl group to the side-chain of Ser53. The other, proximal arginine residue, shows clear electron density for its guanidinium group, which binds in a bidentate manner to the carboxyl group of Asp166, and additionally to the hydroxyl group of Thr201. For Asp166, which is invariantly conserved among all protein kinases, a role in catalysis is suggested, either as the catalytic base for the phosphotransfer reaction, or as having a function in orienting the substrate hydroxyl group toward the γ-phosphorus for nucleophilic attack. Both of these functions contribute to the substrate binding, corroborated by the fact that mutation of Asp166 to Glu causes an increase in K_m for the peptide, but not in K_m for ATP.[38] Thr201, less conserved, has been disputed about as a sensor for the presence of substrate, together with

Table 2. Structures and PKA Inhibition Data of Novel ARC-Type Compounds (First Set)

compd no.	nucleosidic moiety	linker	peptidic moiety	K_d (μM)[b]
1	Adc−	Ahx−	(D-Arg)$_2$-NH$_2$[a]	0.319 ± 0.057
2	Adc−	Ahx−	OH[a]	55.8 ± 0.8
3	Adc−	Ahx−	NH$_2$[a]	2.18 ± 0.09
4	Ado(C=O)−	Abu−	NH$_2$[a]	98.7 ± 1.5
5	Ado(C=O)−	Ahx−	NH$_2$[a]	52.1 ± 1.3
6	Adc−	Ahx−	(D-Arg)-NH$_2$[a]	0.249 ± 0.049
7	Adc−	Ahx−	(D-Lys)-NH$_2$[a]	0.443 ± 0.011
8	Adc−	Ahx−	NH(CH$_2$)$_2$NH$_2$	8.23 ± 0.78
9	Adc−	Ahx−	NH(CH$_2$)$_3$NH$_2$	6.05 ± 0.52
10	Adc−	Ahx−	NH(CH$_2$)$_4$NH$_2$	1.64 ± 0.31
11	Adc−	Ahx−	NH(CH$_2$)$_2$OH	18.7 ± 0.4
12	Adc−	Ahx−	NHBz	13.5 ± 0.6
13	Adc−	Ahx−	[L-Phe(Bzo)]-NH$_2$[a]	over 100
14	Adc−	Ahx−	[D-Phe(Bzo)]-NH$_2$[a]	1.96 ± 0.32

[a] −OH stands for a carboxylic group and −NH$_2$ for an amide group at the C-terminus of the inhibitors. [b] Measured in fluorescence polarization assay.[40]

Table 3. Structures and PKA Inhibition Data of Novel ARC-Type Compounds (Second Set)

compd no.	nucleosidic moiety	first linker	chiral spacer	second linker	peptidic moiety[a]	K_d (nM)[b]
15	Adc−	Ahx−	(D-Lys)−	Ahx−	(D-Arg)$_2$-NH$_2$	7.6 ± 0.1
16	Adc−	Ahx−	(D-Lys)−	Abu−	(D-Arg)$_2$-NH$_2$	12.6 ± 0.1
17	Adc−	Ahx−	(D-Lys)−	Aoc−	(D-Arg)$_2$-NH$_2$	9.5 ± 0.1
18	Adc−	Ahx−			Ahx−	(D-Arg)$_2$-NH$_2$	83.0 ± 1.4
19	Adc−	Ahx−			Abu−	(D-Arg)$_2$-NH$_2$	247 ± 11
20	Adc−	Ahx−			Aoc−	(D-Arg)$_2$-NH$_2$	95.4 ± 0.9
21	Adc−	Ahx−	(D-Lys)−	Ahx−	(D-Arg)$_4$-NH$_2$	∼0.5
22	Adc−	Ahx−	(D-Lys)−	Ahx−	(D-Arg)$_6$-NH$_2$	below 0.5
23	Adc−	Ahx−	(D-Lys)−	Ahx−	(L-Arg)$_2$-NH$_2$	8.7 ± 0.5
24	Adc−	Ahx−	(L-Lys)−	Ahx−	(D-Arg)$_2$-NH$_2$	594 ± 12
25	Adc−	Ahx−	(D-Ala)−	Ahx−	(D-Arg)$_2$-NH$_2$	5.8 ± 0.1

[a] −NH$_2$ stands for amide group at the C-terminus of the inhibitors. [b] Measured in a fluorescence polarization binding/displacement assay.

Asp166.[39] Another contact from the peptidic part of the inhibitor, although less defined, is from O77 to the ammonium group of Lys168—this residue is invariantly conserved in the Ser/Thr subfamily of protein kinases and is important for catalysis.[36]

Prior to cocrystallization experiments, there was some expectation that the two arginine residues of the compound **1** might have a similar positioning and function as the two Arg residues (P-2 and P-3) in the PKA substrate's consensus sequence, Arg-Arg-Xaa-Ser/Thr-Yaa. There is no indication, however, of a direct interaction of the arginines of the compound **1** with the known substrate recognition residues of PKA, i.e., Glu127, Glu170, and Glu230. In this respect, the compound **1** seems only in part to represent the previously reported ARC-type inhibitors of high potency,[7,20] which contain four or six arginines. A possible scenario is that the first two D-arginine residues of the conjugates with 4 or 6 arginines provide suitable stereochemical geometry to serve as a joining chain between the linker and the C-terminal arginines, which then are responsible for the interaction with basophilic kinases, including PKA.

Rational Design of Inhibitors. On the basis of the crystal structure of the PKA Cα−compound **1** complex, we designed and synthesized two sets of novel ARC-type inhibitors.

The crystal structure indicates a certain conformational mobility of the arginine moieties of the compound **1**, with the exception of the guanidinium group of the proximal arginine residue, which is bound to the enzyme. This suggests that a significant contribution to the binding is provided by the Ahx linker moiety, at least in the case of compounds with short peptidic moieties. To test the role of the linker for binding, we designed a set of derivatives either without any peptide portion or with different amine or amino acid extensions.

The compounds of the first set (Table 2) have all an adenosine-4′-dehydroxymethyl-4′-carboxylic acid or -carbamoyl moiety attached to the N-terminus of Ahx linker (compounds **2**−**5**), and 1−2 small amine or amino acid moieties connected to the C-terminus of the linker (compounds **6**−**14**).

Within this set, we also tested the tolerance of PKA for a negative charge at the C-terminus of the linker (the compound **2**) and tested the effect of the structure of adenosine−linker connection without changing the total length of the conjugate (compound **4**) or without changing the structure of the linker (compound **5**).

Two additional aspects were explored. PKA Cα has a preference for substrates or pseudosubstrates incorporating basic

amino acid residues. Therefore, we tried the effect of basic amino acids (compounds **6**−**7**), aliphatic amines and diamines, and/or hydrogen bond donors (compounds **8**−**11**) on inhibitory potency and affinity of the conjugates. Second, PKA has a hydrophobic P + 1 pocket, which in the crystal structure is positioned near the C-terminus of the inhibitor. Therefore, to analyze possible binding of inhibitors with C-terminal aromatic groups to the aromatic rings of Phe54 and Phe187, we inserted aromatic amines/amino acids (compounds **12**−**14**) as moieties to the C-terminus of the linker.

The second set of inhibitors (compounds **15**−**25**, Table 3) was designed to afford hydrogen bonds and charge−charge interactions between the arginine residues of the peptidic part of the inhibitors and the peptide substrate or pseudosubstrate recognition site of PKA Cα that is known to include glutamate residues Glu127, Glu170, Glu230, and Glu203. The former three glutamate residues usually interact with the P-2, and P-3 arginine residues in the consensus sequence of PKA substrates and pseudosubstrates; Glu203 interacts with the P-6 arginine residue of the protein kinase inhibitor PKI.[41] In the crystal structure of PKA Cα−compound **1**, the arginine residues do not interact with any of these specific glutamate residues. Three of the glutamate residues are too far away for an interaction, only Glu170 theoretically could be within reach of one of the two arginine residues, but apparently such an interaction is not favored. Thus, we decided to elongate the linker part of the conjugates by introducing a second linker. The conformation of the arginine moieties of the compound **1** in the crystal structure points to the possibility that the peptidic part could serve as a suitable chiral spacer for the binding of the conjugates incorporating longer peptides. Hence, in compounds **15**−**20** we varied the length of the second linker and checked whether the chiral spacer between the two linkers could affect the binding. We used a lysine residue as the chiral spacer, a conservative replacement for arginine and, from the future prospective, suited for the attachment of various cargoes to the conjugate via its amino group. We have also tested the effect of the L-enantiomers of amino acid residues in the peptidic moiety (compound **23**) or the chiral spacer (compound **24**). In compound **25**, a D-alanine residue was used as the chiral spacer to assess the effect of side-chain functionality of the chiral spacer on the affinity of the inhibitor.

The best ARC-type inhibitors reported so far contained six D-arginine residues,[7,20] therefore, in compounds **21** and **22**, we increased the number of arginine residues to four and six, respectively.

Biological Evaluation of the Inhibitors. Out of the 14 compounds from the first set of inhibitors (Table 2), the best inhibition constants were measured for compounds **6** and **7**

featuring D-arginine and D-lysine at the C-terminus of the inhibitor (K_d of 249 and 443 nM, respectively). This result matches with the observed enzyme contacts of the guanidinium group of the first arginine residue of the compound **1** in the crystal structure—i.e., to the carboxylate group of Asp166 and to Thr201. The interpretation was further supported by the observed tendency of compounds **8−10** to show increasing affinity when the distance between the end of the linker and the protonated amine group increases (K_d 8.23 μM for compound **8** versus K_d 1.64 μM for compound **10**). Possibly, the hydrogen bonds and ionic interactions of the ammonium group with the carboxylate group of Asp166 are favored in case of longer and more flexible chain. The preference for a positive charge in this region of the inhibitor is further supported by a 2-fold increase in K_d value when the hydroxyl group is substituted for the amine group (compound **11**) compared to the corresponding amine-containing counterpart (compound **8**).

Considering the small molecular weight of the compound **3** (MW = 394.2, see Supporting Information), it possesses a remarkable K_d value of 2.18 μM (binding energy approximately 0.28 kcal per heavy atom). In contrast, its carboxylate counterpart (compound **2**) has a 25-fold higher K_d. There is no obvious explanation for this effect of the negatively charged group on binding affinity, as the crystal structure does not elucidate any obvious advantage of an amide group over a carboxylate group. Thus, right now it cannot be excluded that the carboxyl group at the C-terminus of the linker may form interactions to amino acids of PKA C that change the binding pattern of the inhibitor while decreasing its net affinity. A possible "candidate" for such an interaction could be Lys72 of PKA C; in the crystal structure of PKA Cα−compound **1**, however, it lies 6.46 Å away from the nitrogen of the amide group of the compound **1**, a closer contact would most certainly require differences in the binding pattern of the linker region.

The positioning of the carbonyl group between ribose and the linker (compound **4** versus compound **3**) is also very important. In compound **4**, the carbonyl is located two bonds further away from the ribose. Obviously, this change causes the loss of the water-mediated interactions to Lys72 and Thr183, which results in weakening of the interaction. Further, the plane formed by C4′, C5′O5′, and the amide group of the linker is shifted in position by two carbon atoms. The curvature of the flexible linker underneath the glycine flap, as observed in the PKA−compound **1** structure, which occurred probably also in case of the compound **3**, is interrupted in the compound **4** by the insertion of the planar carbamoyl group; it is likely that this will result in a change of the interactions of the linker with the glycine flap, possibly leading to the lower binding affinity found for the compound **4**. The compound **5**, being analogical to compound **4** in the nucleosidic part but incorporating aminohexanoic acid moiety as a linker and hence endowed with a possibility to develop interactions with Gly-rich flap probably analogical to the compound **1**, demonstrated 2-fold lower K_d value than the compound **4**. Thus, Ahx moiety served as the optimal linker in all compounds of the given set.

In the case of the compound **12**, the incorporation of an aromatic moiety to the C-terminus of the linker resulted in a 6-fold increase of K_d compared to the compound **3**. The aromatic group was introduced to utilize possible hydrophobic interactions with aromatic amino acid residues of PKA, namely Phe54 and Phe187. Apparently, this requires a larger distance from the linker as shown with the compound **14**, where the incorporation of a more bulky aromatic system (para-benzoyl-D-phenylalanine) is tolerated very well. The use of the L-counterpart (compound

13), however, increases the K_d dramatically, which points to the steric conflicts caused by change of the stereochemistry.

These results demonstrate the great sensitivity of the efficiency of the interaction with PKA C to changes in the inhibitor linker region, both at its N-terminus and C-terminus. The highest affinity of the conjugate is achieved when the 6-aminohexanoic acid linker (Ahx) is attached to the carboxyl group of the nucleosidic fragment, adenosine-4′-dehydroxymethyl-4′-carboxylic acid. Basic amino acids (especially arginine) or aromatic residues big enough to protrude to the hydrophobic pocket are preferred at the C-terminus of the conjugate. The stereochemical configuration of the residue inserted directly C-terminal from the linker seems extremely important; D-amino acids are strongly preferred over L-isomers here.

The largely different positioning of the two arginine residues of the compound **1** from these of the P-3 and P-2 arginine residues of basic protein/peptide substrates and pseudosubstrates in the complex with PKA Cα points to possible benefits of elongation of the linker region of the conjugate. In agreement with this, the K_d value of the compound **15** (K_d = 7.60 nM), which possesses two linkers and D-lysine as the chiral spacer, is over 30-fold lower than that of the compound **6**. The comparison of the affinities of the compounds **15−17** indicates that the 6-aminohexanoic acid residue has an optimal length for the "second" linker. The Ahx linker thus may facilitate an interaction of the arginine residues from the peptidic part of inhibitor with the acidic peptide recognition residues of the enzyme (i.e., Glu127, Glu170, Glu203, or Glu230).

The significantly lower inhibitory potency of the compounds **18−20** compared to their counterparts with an additional D-lysine residue as the spacer between the two linker moieties (compounds **15−17**) reveals the importance of such a chiral spacer. The requirement for the defined stereochemistry is further demonstrated by the much lower binding affinity of the compound **24**, which contains L-lysine (K_d = 594 nM) instead of D-lysine of the compound **15** (K_d = 7.60 nM). In the peptidic part of the inhibitor, however, L-amino acid residues are tolerated quite well, as indicated by the binding characteristics of the compound **23**. D-Amino acid-containing compounds, however, are generally preferred in inhibitor design because their incorporation makes compounds more stable against proteolytic degradation.[7] Compound **25** with D-alanine as the chiral spacer showed slightly better binding characteristics than the corresponding D-lysine containing compound **15**. This indicates that in case of longer conjugates, the stereochemical nature of the spacer that disposes the second linker and the C-terminal D-arginine residues is more important than the direct interaction of the spacer with the enzyme, supposedly with residues Asp166 and Thr201.

Finally, the conjugates **21** and **22**, incorporating adenosine-4′-dehydroxymethyl-4′-carboxylic acid as nucleoside moiety, two linkers, D-lysine as the chiral spacer and four and six D-arginine residues in the peptidic moiety, respectively, had inhibition constants well into the subnanomolar range. Hence, the inhibitory potency of these ARC-type inhibitors reaches that of the best inhibitors of PKA reported so far.[42] Overall, the inhibitors developed in the present work demonstrate the advantages of the rational design based on structures of cocrystals. For example, the most potent of novel ARC-inhibitors (the compounds **21** and **22**) possess approximately 1000-fold higher inhibitory potency toward their biological target PKA C, compared to the compounds designed with the aid of the recently described method of stepwise combinatorial

Table 4. Activity Data of ARC-Type Compounds[a]

compd no.	K_d, PKA (nM)[c]	K_d, ROCK-II (nM)[c]	IC$_{50}$, PKA (nM)	IC$_{50}$, PKBγ (nM)
H89	23 ± 2	31 ± 3	100 ± 20[d] 850 ± 90[e]	662 ± 6[d]
1 (ARC-1034)	319 ± 57		2,600 ± 300[d]	
ARC-902[b]			8.3 ± 1.5[d] 109 ± 21[e]	36.9 ± 2.3[d]
ARC-903[b]			5.3 ± 0.7[d] 67 ± 19[e]	30.7 ± 8.2[d]
ARC-659−1b[b]			2.41 ± 0.10[d] 12.9 ± 2.0[e]	43.1 ± 4.4[d]
3	2180 ± 90	4480 ± 260	26000 ± 1000[d]	over 1000000[d]
6	249 ± 49	89.7 ± 2.4	2100 ± 500[d]	1610 ± 110[d]
15	7.6 ± 0.1	1.4 ± 0.1	54 ± 6[d]	774 ± 13[d]
21	~0.5	below 1	13.4 ± 2.0[e]	56.6 ± 1.0[d]
22	below 0.5	below 1	5.32 ± 0.03[e]	14.6 ± 0.4[d]
25	5.8 ± 0.1	119 ± 3	97 ± 9[d]	3,750 ± 100[d]
26	1.8 ± 0.5	187 ± 3	21.1 ± 2[d]	2,038 ± 480[d]

[a] The binding constants were determined by fluorescence-polarization binding/displacement assay with PKA and ROCK-II and inhibition characteristics by fluorometric TLC assay with PKA and PKBγ. [b] Previously reported compounds,[7,20] see structures in Supporting Information. [c] Measured in fluorescence polarization binding/displacement assay. [d] Measured in fluorometric TLC-supported inhibition assay at 100 μM ATP and 30 μM TAMRA-Kemptide or 10 μM TAMRA labeled AKT/PKB/Rac-protein kinase substrate concentration. [e] Measured in fluorometric TLC-supported inhibition assay at 1 mM ATP and 30 μM TAMRA-Kemptide or 10 μM TAMRA-PKB substrate concentration.

Figure 6. Sequence alignment of the kinase regions of PKA, ROCK-I, and ROCK-II. The loops of PKA and the corresponding regions of the Rho-associated kinase isoforms are colored as follows: gray, glycine-rich loop; green, linker responsible for binding of nucleoside moiety of ATP; yellow, catalytic loop; red, Mg-positioning loop; cyan, activation loop; magenta, hydrophobic P + 1 pocket.

evolution for the development of Akt/PKB bisubstrate inhibitors (K_i = 260 nM).[43]

Comparison of Binding and Inhibitory Properties of ARC-Inhibitors in Assays with PKA, PKBγ, and ROCK-II. The inhibitory and binding properties of several novel ARC-type compounds were analyzed, in addition to PKA, also with two other AGC-kinases, PKBγ, and ROCK-II. For comparison, three previously reported potent ARC-type inhibitors ARC-902, ARC-903, and ARC-659−1b were included in the analysis and their inhibitory potency toward PKA and PKBγ was determined (Table 4). For PKA, H89 was used as a reference inhibitor with dissociation constant value determined by fluorescence-polarization binding/displacement assay (K_d = 23 nM), fitting well into the range of inhibition constants reported for this inhibitor (K_i = 6.1 nM,[44] K_i = 48 nM[45]).

Despite the kinase-specific sequence differences in the ATP-binding pockets of ROCK-II and PKA (Leu49, Val123, Glu127, Thr183 in PKA versus Ile98, Met172, Asp176, Ala231 in

ROCK-II),[24] the K_d values for binding of the compound 3 were quite similar for both enzymes.

Crystal structures are available for ROCK-I with various small molecule inhibitors. In the kinetic analysis, ROCK-II instead of ROCK-I was used; however, 92% of the residues constituting the kinase domains are conserved between the two isoforms[46] (Figure 6). Overlay of the crystal structures of PKA Cα−compound 1 and ROCK-I−Fasudil (PDB 2ESM) does not suggest more major interactions between specific amino acid residues of ROCK and the non-nucleosidic part of the compound 1 molecule than for Ser53 (PKA), which is alanine in both ROCK-isoforms. Formation of a weak hydrogen bond between Ser53 and the carbonyl group between two arginine moieties in the compound 3 would not be possible in ROCK (Figure 7). The absence of significant differences is in agreement with the similar K_d values of the compound 3 with both kinases.

The compounds 6 and 15 demonstrate 3−5-fold better binding characteristics for ROCK-II than for PKA. The common feature
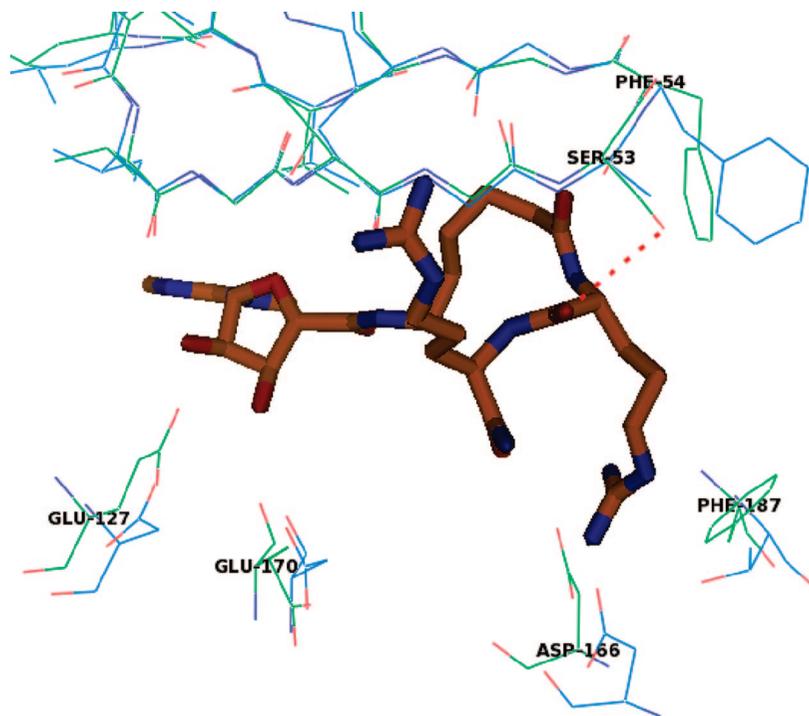
Figure 7. Overlay of crystal structures of PKA Cα−compound **1** (green, the compound **1** is shown with orange carbon atoms) and ROCK-I−Fasudil (PDB 2ESM, blue). Alignment of residues Thr48-Leu59 of PKA and Val81-Leu92 of ROCK-I; the hydrogen bond between the carbonyl of the first arginine of the compound **1** and the side-chain of Ser53 is shown. The residues are labeled according to PKA numbering.

of these compounds is the presence of a D-amino acid residue (arginine or lysine) following the linker moiety. This makes it likely that this residue is involved in ROCK-specific interactions. The comparison of the residues lying near Asp166 of PKA with the corresponding region of ROCK (Figure 6, see catalytic loop) shows a somewhat larger polar pocket in ROCK compared to PKA, which may be suited to accommodate basic moieties of the inhibitors. Also, in PKA, this space is partly filled with the hydrophobic side-chain of Phe187 from the Mg-positioning loop, while ROCK-II has a threonine residue in the corresponding position (Thr235).

In this connection, the binding parameters exhibited by the compound **25** are of special interest. This conjugate, possessing D-Ala residue as the chiral spacer, has over 20-fold higher K_d value for ROCK-II than for PKA. This further supports the conclusion that the lysine spacer inserted between the linkers in the compound **15** gives a specific binding interaction with ROCK-II.

Compounds **21** and **22** exhibit good binding to both PKA and ROCK, and due to the high affinity of the conjugates it is not possible to determine the exact K_d values. The arginine residues lying close to the C-terminus of the inhibitor probably form more potent interactions with PKA, as both kinases recognize arginines/lysines at substrate positions P-2 and P-3, but the residues at positions P-5 and P-6 are more important for binding to PKA C than to ROCK.[47,48]

Thus, it can be concluded that the structure of the linker moiety and the origin of the basic amino acid residue positioned directly after this linker are the most critical features for binding of the inhibitor to ROCK. The introduction of a small, preferably hydrophobic, residue as the first residue after the linker makes the compounds selective for PKA.

Inhibition constants were determined in fluorometric TLC assays[35] with PKA and PKBγ. For PKA, the IC_{50} value for inhibiting the phosphorylation reaction by the compound **6** is 2.1 μM, which is almost equal to that of the compound **1** (IC_{50} = 2.6 μM) within the limits of experimental error. This result is in agreement with the electron density map of the PKA Cα−compound **1** complex that showed missing density for the amide terminus of the molecule and only partial density for the distal arginine of the compound **1**, which most likely indicates that the latter is not bound strongly to PKA C molecule and does not develop significant hydrogen bonds or van der Waals interactions with the glycine flap of PKA C. In the case of the most potent compounds (**21** and **22**), 1 mM concentration of ATP was used in the assay with PKA in order to avoid tight-binding conditions ($IC_{50} \leq C_{kinase}$) and to scale the IC_{50} values to the reasonable range, allowing assessment of the inhibitory properties more precisely. The best inhibitory characteristics belong to the compound **22** that inhibited PKA with an IC_{50} value of 5.3 nM at 1 mM concentration of ATP, resulting in 2-fold better inhibition for PKA C than that previously reported for the most potent ARCs.[7,20]

The IC_{50} value determined by fluorometric TLC method[35] for inhibition of PKBγ by Hidaka's inhibitor H89 was 662 nM. This is comparable to the IC_{50} value reported in the literature for another PKB/Akt isoform PKBβ (IC_{50} = 590 nM for inhibition of PKBβ by H89).[49] The sequence identity is over 80% between PKBβ and PKBγ[50] (Figure 8). Our previously reported ARC-compounds exhibited 5-fold lower IC_{50} values for PKA compared to PKBγ, with the exception of the deoxy-compound ARC-659−1b, which showed more than 10-fold selectivity for PKA over PKBγ.

Surprisingly, compound **3** exhibited extremely poor inhibition of PKBγ, with millimolar IC_{50} value. On the other hand, the addition of one arginine moiety resulted in steep increase of inhibitory potency (the IC_{50} value for PKBγ inhibition by the compound **6** was 1.61 μM). Such a dramatic change points to the different modes of binding of these two inhibitors to the kinase.

The comparison of IC_{50} values for compounds **15** and **25** confirms that PKBγ has preference for a basic residue right after

```
PKA: PUBMED NP_777009
   1 mgnaaaakkg  seqesvkefl  akakedflkk  wenpaqntah  ldqferiktl  gtgsfgrvml
  61 vkhmetgnhy  amkildkqkv  vklkqiehtl  nekrilqavn  fpflvklefs  fkdnsnlymv
 121 meyvpggemf  shlrrigrfs  epharfyaaq  ivltfeylhs  ldliyrdlkp  enllidqqgy
 181 iqvtdfgfak  rvkgrtwtlc  gtpeylapei  ilskgynkav  dwwalgvliy  emaagyppff
 241 adqpiqiyek  ivsgkvrfps  hfssdlkdll  rnllqvdltk  rfgnlkngvn  diknhkwfat
 301 tdwiaiyqrk  veapfipkfk  gpgdtsnfdd  yeeeeirvsi  nekcgkefse  f

PKBβ: PUBMED NP_058789
   1 mnevsvikeg  wlhkrgeyik  twrpryfllk  sdgsfigyke  rpeapdqtlp  plnnfsvaec
  61 qlmkterprp  ntfvirclqw  ttviertfhv  dspdereewi  raiqmvansl  kqrgpgedam
 121 dykcgspsds  stsemmevav  skarakvtmn  dfdylkllgk  gtfgkvilvr  ekatgryyam
 181 kilrkeviia  kdevahtvte  srvlqntrhp  fltalkyafq  thdrlcfvme  yanggdlffh
 241 lsrervfted  rarfygaeiv  saleylhstd  vvyrdiklen  lmldkdghik  itdfglskeg
 301 isdgatmktf  cgtpeylape  vlednqygra  vdwwglgvvm  yemmcgrlpf  ynqdherlfe
 361 lilmeeirfp  rtlgpeaksl  lagllkkdpk  qrlgggpsda  kevmehrffl  sinwqdvvqk
 421 kllppfkpqv  tsevdtryfd  deftaqsiti  tppdrydslg  sleldqrthf  pqfsysasir
 481 e

PKBγ: PUBMED NP_005456
   1 msdvtivkeg  wvqkrgeyik  nwrpryfllk  tdgsfigyke  kpqdvdlpyp  lnnfsvakcq
  61 lmkterpkpn  tfiirclqwt  tviertfhvd  tpeereewte  aiqavadrlq  rqeeermncs
 121 ptsqidnige  eemdastthh  krktmndfdy  lkllgkgtfg  kvilvrekas  gkyyamkilk
 181 keviiakdev  ahtltesrvl  kntrhpflts  lkysfqtkdr  lcfvmeyvng  gelffhlsre
 241 rvfsedrtrf  ygaeivsald  ylhsgkivyr  dlklenlmld  kdghikitdf  glckegitda
 301 atmktfcgtp  eylapevled  ndygravdww  glgvvmyemm  cgrlpfynqd  heklfelilm
 361 edikfprtls  sdaksllsgl  likdpnkrlg  ggpddakeim  rhsffsgvnw  qdvydkklvp
 421 pfkpqvtset  dtryfdeeft  aqtititppe  kydedgmdcm  dnerrphfpq  fsysasgre
```

Figure 8. Sequence alignment of the kinase regions of PKA, PKBβ, and PKBγ. The loops of PKA and the corresponding regions of the PKB isoforms are colored as follows: gray, glycine-rich loop; green, linker responsible for binding of nucleoside moiety of ATP; yellow, catalytic loop; red, Mg-positioning loop; cyan, activation loop; magenta, hydrophobic P + 1 pocket.
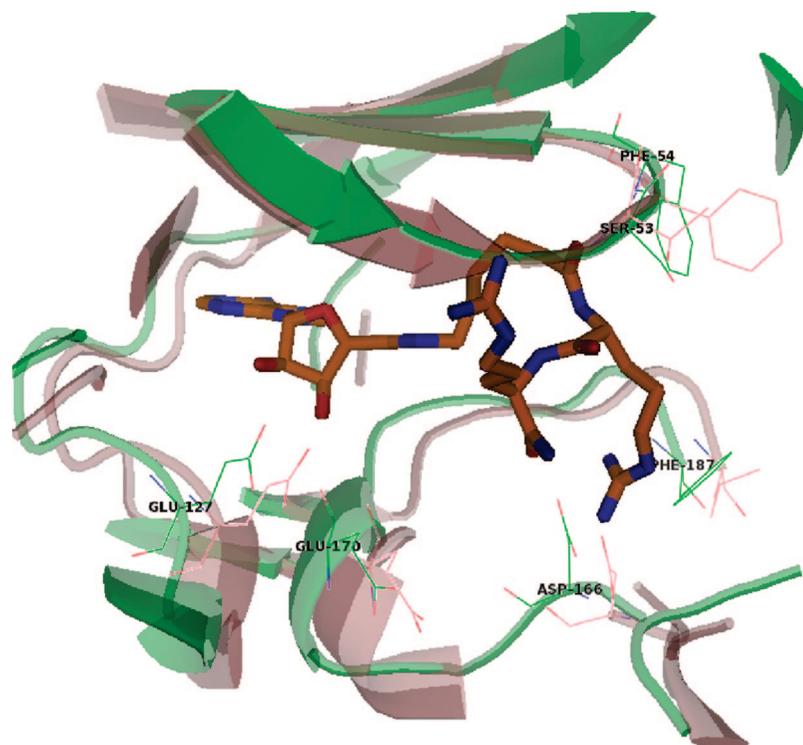

Figure 9. Overlay of crystal structures of PKA Cα−compound **1** (green) and PKBβ complex with H89 and GSK3β (PDB 2JDO, wheat) aligned at PKA residues 48−59 and PKBβ residues 157−168. The compound **1** is shown with orange carbon atoms. The residues are labeled according to PKA numbering.

the first linker. The latter finding could result from the combined effect of several factors, e.g., when Thr165 of PKBγ is substituted for Ser53 of PKA, the first linker of the inhibitor adopts a shifted position favorable for interaction between the basic amino acid residue and Asp278 of PKBγ (Figure 9; the

cocrystal of PKBβ was chosen for the overlay, as PKBγ has not been cocrystallized so far). However, the effect is not as dramatic as in case of ROCK-II.

With the exception of the compound **6**, the novel ARC-inhibitors are less potent toward PKBγ than for PKA, with the

Table 5. Percent of Inhibition of the Protein Kinases in the Presence of Compound **22** (100 nM)

| Protein Kinase	Kinase Group[1]	% Inhibition[a]	Protein Kinase	Kinase Group	% Inhibition
AMPK A1/B1/G1	CAMK	51	PKC α	AGC	94
Aurora A	other	10	PKC βI	AGC	97
CaMK-Iδ	CAMK	35	PKC βII	AGC	94
CaMK-IIα	CAMK	5	PKC δ	AGC	97
CaMK-IIβ	CAMK	16	PKC ε	AGC	106
CDK2/cyclin A	CMGC	0	PKC γ	AGC	107
CHK1	CAMK	88	PKC η	AGC	106
CHK2	CAMK	62	PKC ι	AGC	34
CK1α1	CK1	-30	PKC μ	AGC	54
DAPK3 (ZIPK)	CAMK	22	PKC θ	AGC	97
GSK3α	CMGC	16	PKCζ	AGC	53
GSK3β	CMGC	16	PKD2	CAMK	37
MELK	CAMK	84	PKD3	CAMK	55
MSK1	AGC	105	PKG1	AGC	58
MSK2	AGC	109	PKG2	AGC	16
p70S6K	AGC	96	PRKX	AGC	104
PAK3	STE	74	ROCK-I	AGC	105
PAK4	STE	81	ROCK-II	AGC	104
PAK6	STE	81	RSK1	AGC	98
PDK1	AGC	45	RSK2	AGC	104
PIM1	CAMK	96	RSK3	AGC	99
PIM2	CAMK	79	SGK1	AGC	89
PKA Cα	AGC	104	SGK2	AGC	76
PKBα (Akt1)	AGC	89	SRC	TK	28
PKBβ (Akt2)	AGC	62			
PKBγ (Akt3)	AGC	87			

Legend:
- < 40% Inhibition
- 40% - 80% Inhibition
- ≥ 80% Inhibition

[a] Percent of inhibition of the kinases (at 100 nM concentration of the inhibitor and ATP concentration close to the K_M value of the given kinase toward ATP), as relative to that in control incubations where the inhibitor was omitted (means of duplicate determinations).

greatest difference in case of the compounds **21** and **22**. The inhibitory properties measured in PKBγ inhibition assays were remarkably weaker than in PKA inhibition assays, especially taking into consideration that 10 times lower ATP concentration was used in the assay with PKBγ (100 μM in assay with PKB versus 1 mM in assay with PKA). According to the Cheng−Prusoff equation,[51] a 10-fold increase of ATP concentration results in 10-fold decrease of inhibition constant K_i.

Furthermore, the inhibition constant is also linearly dependent on the K_M for ATP, and the K_M value of PKBγ for ATP (K_M = 88 μM)[52] is ca. 5-fold higher than that for PKA C (K_M = 18.7 μM).[35] Thus, the 3-fold difference of IC$_{50}$ values presented in Table 4 for the inhibition of PKA and PKBγ by most potent novel ARCs (the compounds **21** and **22**) means approximately 150-fold difference in corresponding inhibition constants K_i in favor of PKA.

Finally, to confirm our assumptions about the structural determinants of kinase selectivity of ARC-type inhibitors, we designed the compound **26** (ARC-1044, see Figure 10). The nucleosidic part of the compound **26** is a cyclopentane-based carbocyclic analogue of 3′-deoxyadenosine that, if conjugated with hexa-(D-arginine) (corresponding compound ARC-659−1b), was previously shown to enhance selectivity toward PKA in a panel of 34 protein kinases.[20] The second structural element responsible for selectivity of the compound **26** was D-alanine residue used as the chiral spacer between the linkers.
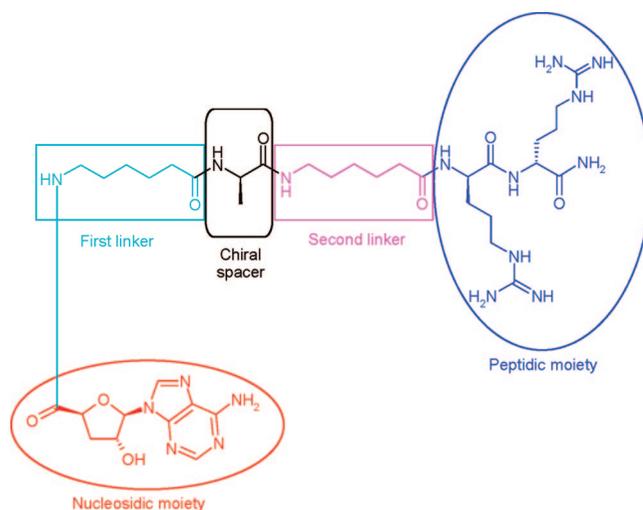
Figure 10. The structure of the compound **26**.

The inhibitory properties of the compound **26** confirmed our predictions, as it exhibited over 100-fold selectivity toward PKA over ROCK-II and PKBγ (Table 4).

Selectivity Studies. Selectivity testing was performed toward a panel of 50 kinases (on commercial basis, Invitrogen SelectScreen Biochemical Kinase Profiling, Z′-LYTE Assay) of the most potent of the novel ARC-type compounds, the
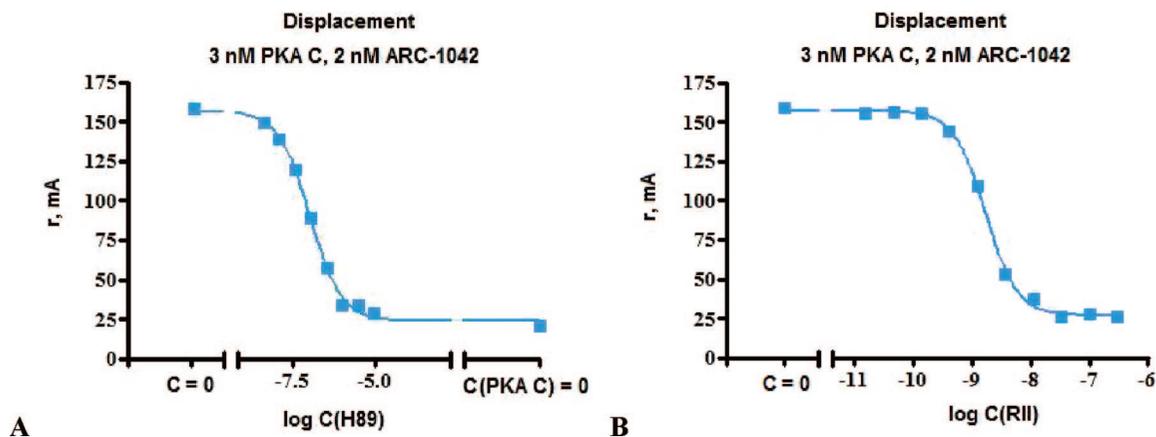
Figure 11. (A) Displacement of compound **27** from its complex with PKA by H89; (B) displacement of compound **27** from its complex with PKA by RIIα. The analogical displacement of compound **27** from its complex with PKA by Ala-Kemptide is presented in the Supporting Information.

compound **22** (Table 5). The kinases were chosen according to our previous knowledge, expecting that the basophilic kinases will constitute the "target group" and the "negative controls" represented by acidophilic CK1, representatives of CMGC group (CDK2, GSK isoforms), and tyrosine kinase Src.

As expected, the compound **22** inhibited most potently the AGC family of basophilic protein kinases and did not inhibit at all the acidophilic casein kinase (CK1). Overall, the most inhibited protein kinases (over 90% inhibition) were PKA C, PKC (except isoforms ι, ζ, and μ), ROCK isoforms, and ribosomal S6-kinases (RSK, MSK, p70S6K), all from the AGC kinase family. PKBα, PKBγ, SGK (all from AGC family), and PAK isoforms (STE family) were also well inhibited (over 80%).

The inhibition preferences of the compound **22** were generally similar to that of previously reported compound ARC-902[7] (possessing six arginine moieties and one linker, kinase screening performed at 1 μM concentration of the inhibitor), although the compound **22** inhibited PKA and PKC isoforms better and the representatives of CAMK family (e.g., CaMK isoforms and PKD) worse than ARC-902.

The inhibition potential of the compound **22** determined for PKA C, PKBγ, and ROCK-II was in agreement with the results of our measurements (Table 4).

Confirmation of the Bisubstrate Character of Novel Inhibitors. Previously, we have demonstrated that the inhibition of PKA by ARC-type inhibitors is competitive with ATP and noncompetitive with the peptide substrate TAMRA-Kemptide.[7] This result probably indicates an ordered mechanism of inhibition where the interaction of the nucleosidic moiety of the bisubstrate-analogue inhibitor with the ATP-binding site is first required to allow the interaction of the peptidic fragment of inhibitor with the protein/peptide-binding site of PKA.[14,18] However, the complete displacement of the ARC-type inhibitor from its complex with PKA C either by ATP or by protein/peptide substrate confirms the bisubstrate character of the inhibitor.[21]

Therefore, we performed the displacement of a novel ARC-type inhibitor from its complex with PKA Cα by either PKA RIIα subunit binding to the peptide substrate site, or ATP-competitive inhibitor H89. A fluorescent probe, compound **27** (ARC-1042, see structure in the Supporting Information), was designed originating from the compound **22** to perform a fluorescence-polarization binding/displacement assay.[40] Compared to the compound **22**, the changes in the structure of

compound **27** were as follows: D-arginine was used as the chiral spacer between the linkers and one D-lysine residue was attached to the C-terminus of the peptidic part of the inhibitor. The fluorescent label 5-TAMRA was fused with the side-chain of D-lysine.

The dissociation constant of 0.3 nM was determined for compound **27** from titration with PKA (see Supporting Information). The high affinity of the fluorescent probe enabled performance of the displacement of compound **27** from the complex with PKA by either H89 (Figure 11A) or PKA RIIα (Figure 11B).

The fluorescent probe could be successfully displaced from the complex with PKA by both H89 (targeted to ATP-binding pocket of ATP) and RIIα (regulatory subunit of PKA, known to compete with protein/peptide substrates), thus proving the bisubstrate character of the fluorescent probe and novel ARC-type inhibitors. The displacement IC$_{50}$ value obtained for RII subunit was 1.69 nM (the corresponding K_d value below 0.3 nM), and the displacement IC$_{50}$ for H89 was 109.6 nM (the corresponding K_d = 11.4 nM).

Conclusions

The crystal structure of the complex PKA Cα−compound **1** demonstrated the principal binding pattern of ARC-type protein kinase inhibitors and paved the way for the rational design of highly potent ARC-type bisubstrate analogues. Structural elements responsible for affinity and selectivity were established using newly synthesized derivatives with corresponding modifications in inhibition and binding assays. A prominent and important feature of the compound **1** molecule is the Ahx linker, joining the nucleosidic and peptidic part of the inhibitor. Its length, shape, and electronic properties together with backbone flexibility are obviously well suited to support multiple favorable interactions with the glycine flap of the kinase, thus providing an explanation for the good inhibitory potency of ARC-type compounds. The elongation of the linker facilitated the interaction of the peptidic part of bisubstrate−analogue inhibitors with those amino acid residues of PKA C that are responsible for substrate consensus sequence recognition. This was achieved by adding the second Ahx-linker. The highest affinity toward PKA C was obtained using the orienting effect of a D-amino acid as the chiral spacer between the two Ahx-moieties. Out of 24 inhibitors synthesized proceeding from the structure of the compound **1** cocrystal, the highest inhibitory potency was obtained for the compounds **21** and **22**, consisting of adenosine-

4′-dehydroxymethyl-4′-carboxylic acid as nucleoside group, two linkers (both 6-aminohexanoic acid moieties), D-lysine as a chiral spacer, and four or six D-arginine residues in the peptidic moiety, respectively. With inhibition constants in the subnanomolar range, they appear to be the highest affinity synthetic small-molecular PKA inhibitors reported so far. Comparison of the inhibitory activity of the novel ARC-inhibitors toward three closely related protein kinases of the AGC group PKA, PKBγ, and ROCK-II from the AGC-group revealed structural elements responsible for the selectivity.

Materials and Methods

Materials. All chemicals were obtained commercially unless otherwise noted. PKA Cα and PKA RIIα for fluorometric TLC assay and fluorescence polarization-based assay was obtained from Biaffin. PKB (Akt3/PKBγ, S472D, active) was obtained from Invitrogen, and 5-TAMRA labeled AKT/PKB/Rac-protein kinase substrate (ARKRERTYSFGHHA) was obtained from Anaspec. Solvents were from Rathburn and Fluka. Fmoc Rink Amide MBHA resin and other peptide synthesis chemicals were from Neosystem, Novabiochem, Advanced ChemTech, and AnaSpec. The synthetic peptide substrate 5-TAMRA labeled Kemptide (LRRASLG) was synthesized as previously described.[35] The other chemicals were from Sigma-Aldrich. ^{1}H and ^{13}C NMR spectra were taken on Bruker AC 200P spectrometer (see Supporting Information). Mass spectra of all synthesized compounds were measured with MALDI-TOF mass spectrometer Voyager DE-Pro (Applied Biosystems) and mass spectra of conjugates **1**−**26** was recorded on Thermo Electron LTQ Orbitrap mass spectrometer (see Supporting Information). Unicam UV 300 (ThermoSpectronic) spectrometer was used for measuring UV−vis spectra and quantification of the products. Fluorescence anisotropy readings were taken on a PHERAstar microplate reader (BMG Labtech) with optic module FP 540−20 590−20. Corning black low volume 384-well NBS plates (code 3676) were used for fluorescence anisotropy readings. The solution-phase reactions were monitored by thin-layer chromatography (TLC) on Polygram Sil G/UV254 plates (Macherey-Nagel), and a UV-lamp was used for the visualization of the products. Fluorescence imaging of TLC plates was performed by Molecular Imager FX Pro Plus (Bio-Rad Laboratories; excitation at 532 nm, 555 nm LP emission filter, 100 μm resolution), and scanned images were processed with Quantity One software (Bio-Rad). Column chromatography was performed on silica gel 60 (0.04−0.063 mm), purchased from Fluka. The final products were purified with Gilson HPLC system using C18 reverse-phase column (GL Sciences) Inertsil ODS-3 (5 μm, 25 cm × 0.46 cm), with monitoring at 260 or 220 nm (peptides). Elution was performed with water−acetonitrile gradient (0.1% TFA) with a flow rate of 1 mL/min. The separated products were freeze-dried. The products **1**−**21** and **23**−**25** were characterized by ion exchange chromatography on Luna SCX 5 μ 150 mm × 4.6 mm column (Phenomenex) by using the eluent systems of A (20 mM phosphate buffer, pH 7.6, 18% isopropanol) and B (40 mM phosphate buffer, pH 7.6, 1.2 M NaCl, 18% isopropanol) with a flow rate of 1 mL/min and detection at 260 nm. Inhibitors **22** and **26** were characterized by ion exchange chromatography on Mono S HR 5/5 column (Pharmacia Biotech) by using the eluent systems of A (20 mM phosphate buffer, pH 7.6, 18% isopropanol) and B (40 mM phosphate buffer, pH 7.6, 1.2 M NaCl, 18% isopropanol) with a flow rate of 1 mL/min and detection at 260 nm. All compounds used in biological tests were >95% pure by HPLC (detected at 260 nm). Concentrations of compounds for biological testing were measured by UV spectroscopy (based on molar extinction coefficient of 15000 M^{-1} cm^{-1} at 260 nm for adenosine derivatives).

Protein Expression and Purification. Bovine wild-type Cα catalytic subunit of the cAMP-dependent protein kinase was solubly expressed in *Escherichia coli* BL21(DE3) cells and then purified via affinity chromatography and ion exchange chromatography as previously described.[29] Constitutively active bovine GST-Rho-kinase (ROCK-II, amino acids 6−553) was purified from Sf9 cells

by use of a baculovirus system[53] by means of a glutathione-Sepharose column.

Crystallization. The compound **1** was cocrystallized with bovine Cα catalytic subunit of the cAMP-dependent protein kinase using the hanging drop vapor diffusion method. Droplets contained 18 mg/mL protein, 25 mM Mes-BisTris, 75 mM LiCl, 1 mM dithiothreitol, pH 6.1−6.8, and 1.5 mM inhibitor and were equilibrated at 4 °C against 13−20% (v/v) methanol.

Data Collection and Structure Determination. Diffraction data were measured from frozen crystals at the beamline BW6, Deutsches Elektronen Synchrotron (DESY), Hamburg. The data were processed with the programs MOSFLM and SCALA. The structures were determined by molecular replacement using AMoRe from the CCP4 program suite (www.ccp4.ac.uk/main/html). As the search model, we chose a binary PKA−PKI(5−24) complex, omitting the peptide in the search coordinates (unpublished). The structure was refined by one round of rigid body refinement and repetitive rounds of restrained refinement using Refmac5. Model building was performed using the ligand builder tool of the CCP4 suite and Moloc (www.moloc.ch). Phosphorylation sites were found at Ser-139, Thr-197, and Ser-338. Water molecules were automatically inserted using the CCP4 programs PEAKMAX and WATPEAK and visually inspected. Finally, the inhibitor molecules were built and modeled into the inner and the outer difference electron densities, and the whole complex was further refined.

Structural Analysis. For a visual inspection of the crystal structure and comparison of conformational changes, structures were aligned using the programs Moloc and Pymol (www.pymol.org). Figures were prepared with Moloc or Pymol.

Chemical Synthesis. Inhibitors **1**, **3**−**6**, and **13**−**26** were synthesized by Fmoc solid phase peptide synthesis strategy and purified by reverse phase HPLC as previously described.[7,35] The synthesis of peptide fragments was carried out on Fmoc Rink Amide MBHA resin. Protected amino acids (3 equiv, Pbf and Boc as side-chain protective groups for arginine and lysine, respectively) were dissolved in DMF/NMM and activated with HOBT/BOP mixture (2.9 equiv). The coupling solutions were added to the resin and agitated for 90 min. Completeness of each reaction was monitored by Kaiser test, followed by deprotection of Fmoc group with 20% piperidine in DMF (20 min). Fmoc-protected linkers were attached to the peptide following the same protocol. The nucleoside part was introduced by application of either 2′,3′-*O*-isopropylideneadenosine-4′-dehydroxymethyl-4′-carboxylic acid (1.5 equiv) solution in DMF/DIEA after activation with HOBT/BOP (1.47 equiv) or in case of the compounds **4** and **5** by 4′-nitrophenyloxycarbonylimino-4′-dehydroxymethyl-2′,3′-*O*-isopropylideneadenosine (1.2−1.3 equiv) solution in DMF/DIEA. In the former case, three-hour reaction time was used, whereas in the latter case, the reaction mixture was agitated overnight. The washing procedure with three solvents (DMF, isopropanol, DCE) followed and after freeze-drying the derived resin was treated with cleavage cocktail (TFA/TIPS/H$_2$O mixture) for 2.5 h. The collected product was evaporated to dryness, washed with methyl-*tert*-butyl ether, and subjected to further purification by HPLC.

The precursor reagents of inhibitors **2** and **8**−**12** were synthesized in solution and the corresponding full schemes of synthesis are presented in the Supporting Information.

Fluorometric TLC Kinase Assay. The IC$_{50}$ values of the inhibitors corresponding to the concentration of the inhibitor decreasing the enzyme activity 2-fold were measured as previously described.[35] The inhibitors in various concentrations were incubated at 30 °C in Hepes buffer (50 mM, pH 7.5) containing PKA Cα (1 nM) or PKBγ (0.5 nM), TAMRA-Kemptide (30 μM) or TAMRA-labeled AKT/PKB/Rac-protein kinase substrate (10 μM), ATP (100 μM or 1 mM in case of inhibitors with very high affinity), magnesium acetate (10 mM), and bovine serum albumin (0.2 mg/mL). The phosphorylation reaction was initiated by the addition of ATP. At fixed time points, the reaction was stopped by a 20-fold dilution with 75 mM phosphoric acid and samples were analyzed by normal phase TLC (without fluorescence indicator, eluted with 1-butanol/pyridine/acetic acid/water, 15/10/12/12 by volume). The

visualization and quantification of the fluorescent spots were carried out by fluorescence imaging. The data were processed with Graphpad Prism software version 4.03.

Fluorescence Polarization-Based Binding/displacement Kinase Assay. All concentration-dependent binding experiments were performed as previously described[40] using 3-fold dilution series in the assay buffer (150 mM NaCl, 50 mM HEPES hemisodium salt pH 7.5, 5 mM DTT, 0.5 g/L BSA) with 10 min incubation time. The concentration of fluorescent ligand was 2 nM, and the concentration of enzyme was 3 nM for PKA and 20 nM for ROCK-II; the final solution volume in the wells was 20 μL. The binding curves were fitted using GraphPad Prism version 4.03 using sigmoidal dose−response variable slope regression functions. The dissociation/displacement constants K_d were calculated with the aid of the online calculator for fluorescence-based competitive binding assays (http://sw16.im.med.umich.edu/software/calc_ki/index.jsp[54]).

Supporting Information Available: View of the total crystal structure of PKA Cα−compound **1** complex, tables listing structures and analytical data of the inhibitors, and descriptions of synthesis routes of inhibitors **2** and **8**−**12** and their precursor compounds. This material is available free of charge via the Internet at http://pubs.acs.org.

References

(1) Manning, G.; Whyte, D. B.; Martinez, R.; Hunter, T.; Sudarsanam, S. The protein kinase complement of the human genome. *Science* **2002**, *298*, 1912–1934.

(2) Breitenlechner, C.; Gassel, M.; Engh, R.; Bossenmeyer, D. Structural insights into AGC kinase inhibition. *Oncol. Res.* **2004**, *14*, 267–278.

(3) Cohen, P. Protein kinases—the major drug targets of the twenty-first century. *Nat. Rev. Drug Discovery* **2002**, *1*, 309–315.

(4) Noble, M. E.; Endicott, J. A.; Johnson, L. N. Protein kinase inhibitors: insights into drug design from structure. *Science* **2004**, *303*, 1800–1805.

(5) Pelech, S. Tracking cell signaling protein expression and phosphorylation by innovative proteomic solutions. *Curr. Pharm. Biotechnol.* **2004**, *5*, 69–77.

(6) Gill, A. L.; Verdonk, M.; Boyle, R. G.; Taylor, R. A comparison of physicochemical property profiles of marketed oral drugs and orally bioavailable anti-cancer protein kinase inhibitors in clinical development. *Curr. Top. Med. Chem.* **2007**, *7*, 1408–1422.

(7) Enkvist, E.; Lavogina, D.; Raidaru, G.; Vaasa, A.; Viil, I.; Lust, M.; Viht, K.; Uri, A. Conjugation of adenosine and hexa-(D-arginine) leads to a nanomolar bisubstrate-analog inhibitor of basophilic protein kinases. *J. Med. Chem.* **2006**, *49*, 7150–7159.

(8) Nam, N.-H.; Lee, S.; Ye, G.; Sun, G.; Parang, K. ATP−phosphopeptide conjugates as inhibitors of Src tyrosine kinases. *Bioorg. Med. Chem.* **2004**, *12*, 5753–5766.

(9) Shen, K.; Cole, P. A. Conversion of a tyrosine kinase protein substrate to a high affinity ligand by ATP linkage. *J. Am. Chem. Soc.* **2003**, *125*, 16172–16173.

(10) Fischer, P. M. The design of drug candidate molecules as selective inhibitors of therapeutically relevant protein kinases. *Curr. Med. Chem.* **2004**, *11*, 1563–1583.

(11) Knight, Z. A.; Shokat, K. M. Features of selective kinase inhibitors. *Chem. Biol.* **2005**, *12*, 621–637.

(12) Parang, K.; Cole, P. A. Designing bisubstrate analog inhibitors for protein kinases. *Pharm. Ther.* **2002**, *93*, 145–157.

(13) Bogoyevitch, M. A.; Barr, R. K.; Ketterman, A. J. Peptide inhibitors of protein kinases—discovery, characterisation and use. *Biochim. Biophys. Acta* **2005**, *1754*, 79–99.

(14) Lawrence, D. S. New design strategies for ligands that target protein kinase-mediated protein−protein interactions. In *Handbook of Experimental Pharmacology, Inhibitors of Protein Kinases and Protein Phosphatases*; Pinna, A. L., Cohen, P. T. W., Eds.; Springer-Verlag: Berlin, 2005; Vol. 167, pp 11−44.

(15) Lienhard, G. E.; Secemski, I. I. P1, P5-Di(adenosine-5′)pentaphosphate, a potent multisubstrate inhibitor of adenylate kinase. *J. Biol. Chem.* **1973**, *248*, 1121–1123.

(16) Parang, K.; Till, J. H.; Ablooglu, A. J.; Kohanski, R. A.; Hubbard, S. R.; Cole, P. A. Mechanism-based design of a protein kinase inhibitor. *Nat. Struct. Biol.* **2001**, *8*, 37–41.

(17) Jencks, W. P. On the attribution and additivity of binding energies. *Proc. Natl. Acad. Sci. U.S.A.* **1981**, *78*, 4046–4050.

(18) Ricouart, A.; Gesquiere, J. C.; Tartar, A.; Sergheraert, C. Design of potent protein kinase inhibitors using the bisubstrate approach. *J. Med. Chem.* **1991**, *34*, 73–78.

(19) Garber, K. The second wave in kinase cancer drugs. *Nat. Biotechnol.* **2006**, *24*, 127–130.

(20) Enkvist, E.; Raidaru, G.; Vaasa, A.; Pehk, T.; Lavogina, D.; Uri, A. Carbocyclic 3′-deoxyadenosine-based highly potent bisubstrate-analog inhibitor of basophilic protein kinases. *Bioorg. Med. Chem. Lett.* **2007**, *17*, 5336–5339.

(21) Viht, K.; Schweinsberg, S.; Lust, M.; Vaasa, A.; Raidaru, G.; Lavogina, D.; Uri, A.; Herberg, F. W. Surface-plasmon-resonance-based biosensor with immobilized bisubstrate analog inhibitor for the determination of affinities of ATP- and protein-competitive ligands of cAMP-dependent protein kinase. *Anal. Biochem.* **2007**, *362*, 268–277.

(22) Taylor, S. S.; Yang, J.; Wu, J.; Haste, N. M.; Radzio-Andzelm, E.; Anand, G. PKA: a portrait of protein kinase dynamics. *Biochim. Biophys. Acta* **2004**, *1697*, 259–269.

(23) Taylor, S. S.; Kim, C.; Vigil, D.; Haste, N. M.; Yang, J.; Wu, J.; Anand, G. S. Dynamics of signaling by PKA. *Biochim. Biophys. Acta* **2005**, *1754*, 25–37.

(24) Bonn, S.; Herrero, S.; Breitenlechner, C. B.; Elbruch, A.; Lehmann, W.; Engh, R. A.; Gassel, M.; Bossemeyer, D. Structural analysis of protein kinase A mutants with Rho-kinase inhibitor specificity. *J. Biol. Chem.* **2006**, *281*, 24818–24830.

(25) Gassel, M.; Breitenlechner, B. C.; Rüger, P.; Jucknischke, U.; Schneider, T.; Huber, R.; Bossemeyer, D.; Engh, R. A. Mutants of protein kinase A that mimic the ATP-binding site of protein kinase B (AKT). *J. Mol. Biol.* **2003**, *329*, 1021–1034.

(26) Gassel, M.; Breitenlechner, C. B.; König, N.; Huber, R.; Engh, R. A.; Bossemeyer, D. The protein kinase C inhibitor bisindolyl maleimide 2 binds with reversed orientations to different conformations of protein kinase A. *J. Biol. Chem.* **2004**, *279*, 23679–23690.

(27) Breitenlechner, C.; Gassel, M.; Hidaka, H.; Kinzel, V.; Huber, R.; Engh, R. A.; Bossenmeyer, D. Protein kinase A in complex with Rho-kinase inhibitors Y-27632, Fasudil, and H-1152P: structural basis of selectivity. *Structure* **2003**, *11*, 1595–1607.

(28) Prade, L.; Engh, R. A.; Girod, A.; Kinzel, V.; Huber, R.; Bossemeyer, D. Staurosporine-induced conformational changes of cAMP-dependent protein kinase catalytic subunit explain inhibitory potential. *Structure* **1997**, *5*, 1627–1637.

(29) Engh, R. A.; Girod, A.; Kinzel, V.; Huber, R.; Bossemeyer, D. Crystal structures of catalytic subunit of cAMP-dependent protein kinase in complex with isoquinolinesulfonyl protein kinase inhibitors H7, H8, and H89. Structural implications for selectivity. *J. Biol. Chem.* **1996**, *271*, 26157–26164.

(30) Akamine, P.; Madhusudan; Brunton, L. L.; Ou, H. D.; Canaves, J. M.; Xuong, N. H.; Taylor, S. S. Balanol analogues probe specificity determinants and the conformational malleability of the cyclic 3′,5′-adenosine monophosphate-dependent protein kinase catalytic subunit. *Biochemistry* **2004**, *43*, 85–96.

(31) Breitenlechner, C. B.; Wegge, T.; Berillon, L.; Graul, K.; Marzenell, K.; Friebe, W.; Thomas, U.; Schumacher, R.; Huber, R.; Engh, R. A.; Masjost, B. Structure-based optimization of novel azepane derivatives as PKB inhibitors. *J. Med. Chem.* **2004**, *47*, 1375–1390.

(32) Zhang, X.; Gureasko, J.; Shen, K.; Cole, P. A.; Kuriyan, J. An allosteric mechanism for activation of the kinase domain of epidermal growth factor receptor. *Cell* **2006**, *125*, 1137–1149.

(33) Levinson, N. M.; Kuchment, O.; Shen, K.; Young, M. A.; Koldobskiy, M.; Karplus, M.; Cole, P. A.; Kuriyan, J. A Src-like inactive conformation in the abl tyrosine kinase domain. *PLoS Biol.* **2006**, *4*, 753–767.

(34) Cheng, K. Y.; Noble, M. E.; Skamnaki, V.; Brown, N. R.; Lowe, E. D.; Kontogiannis, L.; Shen, K.; Cole, P. A.; Siligardi, G.; Johnson, L. N. The role of the phospho-CDK2/cyclin A recruitment site in substrate recognition. *J. Biol. Chem.* **2006**, *281*, 23167–23179.

(35) Viht, K.; Vaasa, A.; Raidaru, G.; Enkvist, E.; Uri, A. Fluorometric TLC assay for evaluation of protein kinase inhibitors. *Anal. Biochem.* **2005**, *340*, 165–170.

(36) Bossemeyer, D.; Engh, R. A.; Kinzel, V.; Ponstingl, H.; Huber, R. Phosphotransferase and substrate binding mechanism of the cAMP-dependent protein kinase catalytic subunit from porcine heart as deduced from the 2.0 A structure of the complex with Mn^{2+} adenylyl imidodiphosphate and inhibitor peptide PKI(5−24). *EMBO J.* **1993**, *12*, 849–859.

(37) Zheng, J.; Knighton, D. R.; ten Eyck, L. F.; Karlsson, R.; Xuong, N.; Taylor, S. S.; Sowadski, J. M. Crystal structure of the catalytic subunit of cAMP-dependent protein kinase complexed with MgATP and peptide inhibitor. *Biochemistry* **1993**, *32*, 2154–2161.

(38) Gibbs, C. S.; Zoller, M. J. Rational scanning mutagenesis of a protein kinase identifies functional regions involved in catalysis and substrate interactions. *J. Biol. Chem.* **1991**, *266*, 8923–8931.

(39) Yang, J.; Ten Eyck, L. F.; Xuong, N. H.; Taylor, S. S. Crystal structure of a cAMP-dependent protein kinase mutant at 1.26A: new insights into the catalytic mechanism. *J. Mol. Biol.* **2004**, *336*, 473–487.

(40) Vaasa, A.; Viil, I.; Enkvist, E.; Viht, K.; Raidaru, G.; Lavogina, D.; Uri, A. High-affinity bisubstrate probe for fluorescence anisotropy binding/displacement assays with protein kinases PKA and ROCK. *Anal. Biochem.* **2008**, in press, doi:. 10.1016/j.ab.2008.10.030.

(41) Knighton, D. R.; Zheng, J. H.; Ten Eyck, L. F.; Xuong, N. H.; Taylor, S. S.; Sowadski, J. M. Structure of a peptide inhibitor bound to the catalytic subunit of cyclic adenosine monophosphate-dependent protein kinase. *Science* **1991**, *253*, 414–420.

(42) Schneider, T. L.; Mathew, R. S.; Rice, K. P.; Tamaki, K.; Wood, J. L.; Schepartz, A. Increasing the kinase specificity of k252a by protein surface recognition. *Org. Lett.* **2005**, *7*, 1695–1698.

(43) Lee, J. H.; Kumar, S.; Lawrence, D. S. Stepwise combinatorial evolution of Akt bisubstrate inhibitors. *ChemBioChem.* **2008**, *9*, 507–509.

(44) Miick, S. M.; Jalali, S.; Dwyer, B. P.; Havens, J.; Thomas, D.; Jimenez, M. A.; Simpson, M. T.; Zile, B.; Huss, K. L.; Campbell, R. M. Development of a microplate-based, electrophoretic fluorescent protein kinase A assay: comparison with filter-binding and fluorescence polarization assay formats. *J. Biomol. Screening* **2005**, *10*, 329–338.

(45) Chijiwa, T.; Mishima, A.; Hagiwara, M.; Sano, M.; Hayashi, K.; Inoue, T.; Naito, K.; Toshioka, T.; Hidaka, H. Inhibition of forskolin-induced neurite outgrowth and protein phosphorylation by a newly synthesized selective inhibitor of cyclic AMP-dependent protein kinase, *N*-[2-(*p*-bromocinnamylamino)ethyl]-5-isoquinolinesulfonamide (H-89), of PC12D pheochromocytoma cells. *J. Biol. Chem.* **1990**, *265*, 5267–5272.

(46) Nakagawa, O.; Fujisawa, K.; Ishizaki, T.; Saito, Y.; Nakao, K.; Narumiya, S. ROCK-I and ROCK-II, two isoforms of Rho-associated coiled-coil forming protein serine/threonine kinase in mice. *FEBS Lett.* **1996**, *392*, 189–193.

(47) Shi, J.; Wei, L. Rho kinase in the regulation of cell death and survival. *Arch. Immunol. Ther. Exp.* **2007**, *55*, 61–75.

(48) Kang, J. H.; Jiang, Y.; Toita, R.; Oishi, J.; Kawamura, K.; Han, A.; Mori, T.; Niidome, T.; Ishida, M.; Tatematsu, K.; Tanizawa, K.; Katayama, Y. Phosphorylation of Rho-associated kinase (Rho-kinase/ROCK/ROK) substrates by protein kinases A and C. *Biochimie* **2007**, *89*, 39–47.

(49) Collins, I.; Caldwell, J.; Fonseca, T.; Donald, A.; Bavetsias, V.; Hunter, L. J.; Garrett, M. D.; Rowlands, M. G.; Aherne, G. W.; Davies, T. G.; Berdini, V.; Woodhead, S. J.; Davis, D.; Seavers, L. C.; Wyatt, P. G.; Workman, P.; McDonald, E. Structure-based design of isoquinoline-5-sulfonamide inhibitors of protein kinase B. *Bioorg. Med. Chem.* **2006**, *14*, 1255–1273.

(50) Laine, J.; Künstle, G.; Obata, T.; Noguchi, M. Differential Regulation of Akt Kinase Isoforms by the Members of the TCL1 Oncogene Family. *J. Biol. Chem.* **2002**, *277*, 3743–3751.

(51) Cheng, Y.; Prusoff, W. H. Relationship between inhibition constant (K_i) and concentration of inhibitor which causes 50% inhibition (IC_{50}) of an enzymatic reaction. *Biochem. Pharmacol.* **1973**, *22*, 3099–3108.

(52) Zhang, X.; Zhang, S.; Yamane, H.; Wahl, R.; Ali, A.; Lofgren, J. A.; Kendall, R. L. Kinetic mechanism of AKT/PKB enzyme family. *J. Biol. Chem.* **2006**, *281*, 13949–13956.

(53) Ito, K.; Shimomura, E.; Iwanaga, T.; Shiraishi, M.; Shindo, K.; Nakamura, J.; Nagumo, H.; Seto, M.; Sasaki, Y.; Takuwa, Y. J. Phosphorylation and activation of myosin by Rho-associated kinase (Rho-kinase). *Physiology* **2003**, *546*, 823–836.

(54) Nikolovska-Coleska, Z.; Wang, R.; Fang, X.; Pan, H.; Tomita, Y.; Li, P.; Roller, P. P.; Krajewski, K.; Saito, N.; Stuckey, J.; Wang, S. Development and optimization of a binding assay for the XIAP BIR3 domain using fluorescence polarization. *Anal. Biochem.* **2004**, *332*, 261–273.